J Therm Anal Calorim (2011) 105:937–946
DOI 10.1007/s10973-010-1234-6

Synthetic, spectroscopic, thermal, and structural studies of antimony(III) bis(pyrrolidinedithiocarbamato)alkyldithiocarbonates

H. P. S. Chauhan · Abhilasha Bakshi

Received: 9 September 2010 / Accepted: 1 December 2010 / Published online: 14 December 2010

Abstract An account of the synthesis, spectroscopic, thermal and structural behavior of antimony(III) bis (pyrrolidinedithiocarbamato)alkyldithiocarbonates is presented. The reaction of antimony(III) bis(pyrrolidinedithiocarbamate) chloride with potassium organodithiocarbonate in equimolar ratio yielded the corresponding mixed derivatives of the type $[(CH_2)_4NCS_2]_2SbS_2COR$ [where R = Me, Et, Pr^n, Pr^i, Bu^n, and Bu^i]. These newly synthesized complexes have been characterized by physicochemical [molecular weight determination, melting points, and elemental analysis], spectral [UV, IR, far-IR, NMR (^1H and ^{13}C)], thermal [TG, DTA, and FAB^+ mass], and structural [powder XRD and SEM] studies. Analytical studies leads to purity and structural properties of the synthesized complexes on the other hand powder X-ray diffraction and SEM studies show that multiphase, polycrystalline, and rod-shaped complexes have been formed having nanorange crystallite size and monoclinic crystal system.

Keywords Antimony · Dithiocarbamate · Xanthate · TG and DTA

Introduction

During the past decade the study of mixed sulfur donor ligand complexes with main group metals has made a progressive development due to the development of new analytical and structural techniques [1–3]. Striking structural features exhibited by these class of compounds and diversity of sulfur chelating agents used to prepare new coordination and organometallic complexes has increased rapidly during the past few years [4, 5] and the sustained interest is due to the diverse structural features (ranging from monodentate, bidentate, monomeric to polymeric supramolecular assemblies), fascinating architectures, topologies, and their potential applications in areas such as fast ion conductivity, photocatalysis, electrooptics, sensors, thermoelectrics, as well as various biochemical applications [6–8]. Subtle variations in the nature of the organic substituents on the dithiolate group usually result in different structural motifs. In addition to this, stereochemically active lone pair of electrons present on metal atom results geometries which differ from normal mode.

Pyrrolidine dithiocarbamates which represent a class of antioxidants mediate a wide variety of effects in biological systems [9]. It is a multipotent synthetic compound well known for its metal chelation property [10] and one of the most potent and specific NF-κB inhibitor [11, 12]. In addition to this, xanthates are widely used as additives to lubricating oils, as flotation and complexing agents. Their effect on central nervous system and on redox process on human body as well as their catalytic property toward enzyme activation and inhibition has also been reported [13, 14]. Owing to properties of ligands antimony metal containing compounds are commonly used to treat parasitic infections [15] and exhibit a broad spectrum of chemotherapeutic applications and cytotoxic activities [16].

Thermal degradation of such types of complexes often yields binary metal sulfides as a final decomposition product having important physicochemical properties which makes them attractive for a wide range of commercial applications as in photovoltaic, thermoelectric power generators, and in various optoelectronic and thermoelectric cooling devices [17–21]. Thermal analysis is

H. P. S. Chauhan (✉) · A. Bakshi
School of Chemical Sciences, Devi Ahilya University, Takshashila Campus, Khandwa Road, Indore 452001, India
e-mail: hpsc@rediffmail.com

also helpful to study the chemical structure and thermal parameters of the complexes [22–24]. The study of the structural behavior of the complexes derived from the reaction of main group metals with mixed sulfur donor ligands is a matter of significant importance both for the investigation of the geometries of the compounds as well as their importance as binary metal sulfides formed during decomposition processes.

Experimental

Materials

Ammonium pyrrolidinedithiocarbamates (Fluka) were used as received. Antimony trichloride (E. Merck) was distilled before use. The reactants such as potassium organodithiocarbonate and antimony(III) bis(pyrrolidinedithiocarbamate) chloride were prepared by reported methods [25, 26]. Solvents (benzene, carbondisulfide, alcohols, diethyl ether, chloroform, and dichloromethane) were purified and dried by standard methods before use [27].

Measurements

Melting points were determined on a B10 Tech India melting point apparatus and are uncorrected. Antimony was estimated iodometrically [28] and sulfur was estimated gravimetrically as barium sulfate [28]. Molecular weights were determined cryoscopically in benzene. Elemental analysis (C, H, and N) was performed on a Carlo Erba 1108 C, H, N analyzer at the Sophisticated Analytical Instrumentation Facility, CDRI, Lucknow, India. Infrared spectra were recorded on a Spectrum BX Series in the range 4000–400 cm^{-1} and far-IR spectra were recorded as a Nujol mull over CsI disks using a Magna-IR Spectrophotometer-550 instrument in the range 600–50 cm^{-1}. The UV spectra were recorded in chloroform solution at room temperature on a Shimadzu UV-1700 UV–Vis spectrophotometer within a range 400–200 nm. NMR spectra were recorded in $CDCl_3$ solution on High-resolution multinuclear FT-NMR spectrometer operated at 400.23 and 100.63 MHz for ^{1}H and ^{13}C, respectively. The TG and DTA analyses were carried out in inert atmosphere on Mettler STAR^{e} SW 8.10 model. The FAB^{+} mass spectra were recorded on a Jeol SX 102/Da-600 mass spectrometer/Data System using Argon/Xenon as the FAB gas. Powder X-ray diffraction studies performed on diffractometer system XPERT-PRO using CuK_{α} radiation at a wavelength of 1.54 Å and SEM studies performed on a Jeol JSM 5600 having magnification range ×2500–10 μm and at accelerating voltage of 0.5–30 kV.

Synthesis of antimony(III) bis(pyrrolidinedithiocarbamato)alkyldithiocarbonates

Equimolar amounts of antimony(III) bis(pyrrolidinedithiocarbamate) chloride (2.1 g, 4.66 mmol) and potassium iso-propyl dithiocarbonate (0.78 g, 4.66 mmol) in anhydrous benzene (∼20 mL) and carbon disulfide (∼20 mL) mixture were stirred for ∼4 h at room temperature. Precipitated potassium chloride (0.33 g) was removed by filtration. The solvent was removed under reduced pressure and we get a bright yellow colored solid product which was crystallized in dichloromethane [yield = 2.4 g (95%), m.p. = 160 °C]. All the other derivatives were prepared by adopting similar methods. The pertinent analytical and physicochemical data for these complexes are summarized in Table 1.

Results and discussion

Synthesis

Mixed antimony(III) bis(pyrrolidinedithiocarbamato) alkyldithiocarbonates were synthesized by the reactions of antimony(III) bis(pyrrolidinedithiocarbamate) chloride with potassium organodithiocarbonates in an equimolar ratio in anhydrous benzene and carbon disulfide mixture by stirring at room temperature for ∼4 h (Scheme 1).

All these newly synthesized derivatives are bright yellow-colored solids and are soluble in common organic solvents like chloroform, benzene, dichloromethane, DMF, and DMSO. The elemental analysis and molecular weights were also in accordance with molecular formulae.

UV spectral studies

The UV absorption spectral data of these mixed antimony(III) bis(pyrrolidinedithiocarbamato)alkyldithiocarbonates are listed in Table 2, and tentative assignments of the important characteristic bands were made with the help of earlier publications [29–33], which help us to understand structural properties and bonding of the complexes synthesized. The salient points in the UV spectra of the mixed ligand dithiocarbamate–xanthate complexes are the presence of three bands in a range 200–400 nm. First band appears in a range 246–253 nm is due to intraligand $\pi \rightarrow \pi^*$ transition of the NCS group of the dithiocarbamate moiety and this band partly obscured, the band of xanthate moiety which also appears at 245 nm due to an $n \rightarrow \sigma^*$ electronic transition of the xanthate moiety; therefore, it is rather difficult in mixed dithiocarbamate–xanthate complexes to assign the bands unambiguously to either the dithiocarbamate or the xanthate group [30]. Second band

Table 1 Physical and analytical data of antimony(III) bis(pyrrolidinedithiocarbamato)alkyldithiocarbonates

Comp no.	Compound	Yield/%	M.P./ °C	Color and state	Molecular weight found/calculated	Analysis/% found/calculated				
						C	H	N	S	Sb
1	$[(CH_2CH_2)_2NCS_2]_2SbS_2COCH_3$	91	212	Yellow solid	552/563.54	31.93/31.97	4.42/4.47	4.92/4.97	34.10/34.14	21.55/21.60
2	$[(CH_2CH_2)_2NCS_2]_2SbS_2COCH_2CH_3$	96	157 Dec.	Yellow solid	523/535.53	29.10/29.15	3.95/3.95	5.18/5.23	35.87/35.92	22.68/22.73
3	$[(CH_2CH_2)_2NCS_2]_2SbS_2COCH_2CH_2CH_3$	97	126 Dec.	Yellow solid	535/549.54	30.54/30.59	4.16/4.21	5.04/5.09	34.97/35.01	22.11/22.15
4	$[(CH_2CH_2)_2NCS_2]_2SbS_2COCH(CH_3)_2$	95	160	Yellow solid	537/549.54	30.55/30.59	4.16/4.21	5.04/5.09	34.96/35.01	22.11/22.15
5	$[(CH_2CH_2)_2NCS_2]_2SbS_2COCH_2CH_2CH_2CH_3$	91	212	Yellow solid	552/563.54	31.93/31.97	4.42/4.47	4.92/4.97	34.10/34.14	21.55/21.60
6	$[(CH_2CH_2)_2NCS_2]_2SbS_2COCH_2CH(CH_3)_2$	90	236	Yellow solid	550/563.54	31.92/31.97	4.42/4.47	4.94/4.97	34.11/34.14	21.56/21.60

that appears as a shoulder within a range 310–315 nm is attributed to $\pi \rightarrow \pi^*$ transition of the SCS group. The similar observation has been made for third band which also appears as a shoulder within a range 358–362 nm and attributed to either an $n \rightarrow \pi^*$ transition located on the sulfur atom or a ligand $\rightarrow d$ orbital transition [33].

IR and far-IR spectral studies

IR and far-IR spectral data of these newly synthesized complexes are listed in Table 2. Some notable features exist in the IR spectra of the mixed ligand dithiocarbamate–xanthate complexes are the bands in the region 1200–1300 cm^{-1}; this band is attributed to the asymmetric stretching vibration of the C–O bond in the OCS_2 group. The position of this band indicates that the contribution of the xanthate group to the structure of the complex is less than the corresponding structure of the dithiocarbamate group as alkoxy group is weaker electron donor than the dialkylamino group [30].

The band absorbing in the region 1160–1200 cm^{-1} is assigned to the symmetric stretching vibration of the C–O group. All these complexes show medium to strong intensity absorption bands in the region 1030–1043 cm^{-1} due to C–S stretching vibrations of both diorganodithiocarbamate as well as organodithiocarbonate moieties, indicating the bidentate nature of both ligands used [25, 34]. The band attributed to the stretching vibration of the C–N bond of the dithiocarbamate group absorbs in the region 1434–1462 cm^{-1} while medium to weak band absorbs in the region 280–320 cm^{-1} due to Sb–S bond [26, 29].

^{1}H NMR

The ^{1}H NMR spectral data of antimony(III) bis(pyrrolidin edithiocarbamato)alkyldithiocarbonates exhibited the expected patterns [25, 26, 34, 35] as shown in Table 3, pyrrolidinedithiocarbamate moiety appears as a complex pattern within a range 2.01–2.38 ppm and at 3.44–3.82 ppm for CH_2 and NCH_2 proton resonance, respectively. While xanthate moiety gives different patterns according to alkyl group present. As in the complexes having ethyl and methyl groups show triplet at 1.41–1.45 ppm and a quartet at 4.59–4.64 ppm due to proton resonance of CH_3 and OCH_2 of ethyl group, respectively, and a singlet at 4.2 ppm due to CH_3 of methyl group.

Complexes having *n*-propyl and iso-propyl groups in respective ligand show triplet at 0.98–1.02 ppm due to CH_3 proton resonance, multiplet within a range 1.81–1.86 ppm and again a triplet at 4.49–4.53 ppm due to CH_2 and OCH_2 proton resonance of *n*-propyl, respectively, while in the case of iso-propyl a doublet at 1.40–1.42 ppm and a complex pattern at 5.60–5.66 ppm due to CH_3 and OCH proton

$$\left[(CH_2CH_2)_2NCS_2\right]_2 SbCl + KS_2COR \xrightarrow{\text{Benzene} + CS2} \left[(CH_2CH_2)_2NCS_2\right]_2 SbS_2\,COR + KCl\downarrow$$

Scheme 1 Reaction of antimony(III) bis(pyrrolidinedithiocarbamate) chloride with Potassium organodithiocarbonate in equimolar ratio (Where R = methyl, ethyl, *n*-propyl, iso-propyl, *n*-butyl and iso-butyl)

Table 2 UV nm and IR cm^{-1} spectral data of antimony(III) bis(pyrrolidinedithiocarbamato)alkyldithiocarbonates

Compound	I Band	II Band	III Band	*ν*C–N	*ν*C–S	*ν*C–O–C	*ν*C–O	*ν*Sb–S
1	252.44	310	360	1443 s	1036 s	1244 s	1199 s	316 m
2	253.93	312	362	1443 m	1030 s	1220 m	1187 m	302 w
3	253.96	315	363	1434 s	1035 s	1244 s	1200 s	315 w
4	252.28	314	358	1435 m	1030 s	1220 m	1160 m	280 w
5	252.39	311	361	1436 m	1034 s	1240 m	1191 m	302 w
6	246.02	314	361	1462 s	1043 s	1244 s	1180 m	310 w

resonances appears, respectively. On the other hand *n*-butyl group shows triplet at 0.92–0.97 ppm, a complex pattern at 1.21–1.48 ppm and a triplet 4.53–4.57 ppm due to $CH_3(CH_2)_2$ and OCH_2 proton resonances, respectively, and isobutyl group exhibits a doublet at 0.98–1.00 ppm, a multiplet at 1.21–1.65 ppm, and a doublet at 4.32–4.34 ppm due to CH_3, CH, and OCH_2 proton resonances, respectively.

^{13}C NMR

The proton decoupled ^{13}C NMR spectra as shown in Table 3 were recorded in $CDCI_3$, and assignments were made on the basis of previously reported data. These complexes showed characteristic resonances due to both pyrrolidinedithiocarbamate and alkyldithiocarbonates and in good agreement with previously reported data [25, 26, 34, 35]. Pyrrolidinedithiocarbamate gives characteristic peak within a range 25.66–25.89 ppm due to CH_2, 53.26–53.49 ppm due to NCH_2, and 194.81–195.08 ppm which is due to NCS_2 carbons of dithiocarbamate. On the other hand, these derivatives also exhibit the expected signals due to resonances of the corresponding methyl, ethyl, *n*-propyl, iso-propyl, *n*-butyl, and iso-butyl carbons of organodithiocarbonate moiety as indicated in Table 3 and are fairly comparable with the earlier reported data.

Thermal studies

TG and DTA studies

Thermal behavior of the two synthesized complexes, namely, $[(CH_2CH_2)_2NCS_2]_2SbS_2COCH_2CH_2CH_3$ and $[(CH_2CH_2)_2NCS_2]_2SbS_2COCH(CH_3)_2$ have been analyzed [26] in an inert atmosphere in a range 25–600 °C as shown in Table 4 for both complexes. Thermogravimetric analysis of complexes in which we analyze a change in the weight of the substance as a function of temperature or time indicates formation of metal sulfide as a final decomposition product [28]. In the case of complex $[(CH_2CH_2)_2NCS_2]_2SbS_2COCH_2CH_2CH_3$ in Table 4 we observed three-step weight losses as shown in Fig. 1. First decomposition occurs within a range 25–215 °C in which most of the organic part of the ligand has lost and we get $[(CHCH)_2NCS_2]_2$ and ½ Sb_2S_3 as a remaining fragment. In second step of weight loss remaining part further decompose and we get ½ Sb_2S_3 and –NC– as a decomposition product occur in a range 215–400 °C and in third step as a final decomposition product ½ Sb_2S_3 formed in a temperature range 400–600 °C which is also confirmed by remaining material percentage 29.21 (30.90).

On the other hand complex $[(CH_2CH_2)_2NCS_2]_2SbS_2COCH(CH_3)_2$ shows four step weight losses as shown in Fig. 2, in first step which occur in a range 25–220 °C most of the organic part lost and $[(C–C–C)NCS_2]_2$ and ½ Sb_2S_3 remained as a fragment further loss which occur in 220–345 °C gives ½ Sb_2S_3 and ¼ C_2S as a remaining part. Third step from 345–460 °C in which along with metal sulfide some part of sulfur remained which again lost in fourth and final step of decomposition and we get ½ Sb_2S_3 as a final product in which remaining percent obtained is 27.31 (30.90) which also support formation of metal sulfide as a final product. Thus by the help of thermogravimetry studies of complexes we not only determine purity and thermal stability of the complex but also composition of the complex as well which we observed during different steps of weight losses as a fragment formed in different temperature ranges.

In addition to TG analysis, DTA studies are helpful in order to determine type of reaction which occur during decomposition process as during first decomposition step of complex $[(CH_2CH_2)_2NCS_2]_2SbS_2COCH_2CH_2CH_3$ we get endothermic peak at 165 °C temperature and in second step a sharp endothermic peak appears at 275 °C temperature in Fig. 1, which shows that type of reaction occur

Table 3 ^{1}H and ^{13}C spectral data of antimony(III) bis(pyrrolidinedithiocarbamato)alkyldithiocarbonates

Compound	^{1}H Chemical shifts/ppm	^{13}C Chemical shift/ppm
1	2.03–2.26, m, 8H CH_2 of dtc; 3.44–3.82, m, 8H NCH_2 of dtc; 4.25, s, 3H CH_3 of xan	25.89 CH_2 of dtc, 53.49 NCH_2 of dtc 60.86 CH_3 of xan,
2	1.43, t, 3H CH_3 of xan $j = 7.20$ Hz; 2.02–2.06, m, 8H CH_2 of dtc; 3.79–3.82, m, 8H NCH_2 of dtc; 4.62, q, 2H OCH_2 of xan $j = 7.20$ Hz	13.88 CH_3 of xan, 25.71 CH_2 of dtc 53.29 NCH_2 of dtc, 70.64 OCH_2 of xan 195.08 NCS_2 of dtc
3	1.00, t, 3H CH_3 of xan $j = 6.80$ Hz; 1.81–1.86, m, 2H CH_2 of xan 2.01–2.08, m, 8H CH_2 of dtc; 3.78–3.82, m, 8H NCH_2 of dtc; 4.51, t, 2H OCH_2 of xan $j = 6.80$ Hz	10.26 CH_3 of xan, 21.63 CH_2 of xan 25.66 CH_2 of dtc, 53.26 NCH_2 of dtc 76.25 OCH_2 of xan, 194.84 NCS_2 of dtc
4	1.41, d, 6H CH_3 of xan $j = 6.40$ Hz; 2.01–2.08, m, 8H CH_2 of dtc; 3.78–3.82, m, 8H NCH_2 of dtc; 5.63, complex, 1H OCH_2 of xan $j = 6.40$ Hz	21.32 CH_3 of xan, 25.66 CH_2 of dtc 53.27 NCH_2 of dtc,78.98 OCH_2 of xan 194.81 NCS_2 of dtc
5	0.95, t, 3H CH_3 of xan $j = 6.60$ Hz; 1.21–1.48, m, 2H CH_2CH_3 of xan 1.74–1.96, m, 2H CH_2CH_2 of xan; 2.03-2.38, m, 8H CH_2 of dtc 3.66–3.80, m, 8H NCH_2 of dtc; 4.5, t, 2H OCH_2 of xan $j = 6.60$ Hz	13.74 CH_3 of xan, 19.15 CH_2 of xan 25.83 CH_2 of dtc, 30.67 CH_2 of xan 53.44 NCH_2 of dtc, 74.92 OCH_2 of xan 194.88 NCS_2 of dtc
6	0.96, d, 6H CH_3 of xan $j = 6.60$ Hz; 1.00–1.96, m, 1H CH of xan; 2.03–2.38, m, 8H CH_2 of dtc; 3.78–3.82, m, 8H NCH_2 of dtc; 4.3, d, 2H OCH_2 of xan $j = 6.60$ Hz	19.15 CH_3 of xan, 25.83 CH_2 of dtc 30.95 CH of xan, 53.43 NCH_2 of dtc 81.03 OCH_2 of xan, 194.89 NCS_2 of dtc 223.25 OCS_2 of xan

Table 4 Thermal analysis TG and DTA of antimony(III) bis(pyrrolidinedithiocarbamato)*n*-propyldithiocarbonates and antimony(III) bis(pyrrolidinedithiocarbamato)iso-propyldithiocarbonates

TG				DTA	
Step	Temperature range/°C	Different loss % found/calculated	Remaining fragments	Temperature	Type of reaction
I	25–215 A, 25–220 B	17.06/17.23/A	$[(CHCH)_2NCS_2]_2$ + ½ Sb_2S_3 A	165 °C A	Endothermic A
		23.35/23.36/B	$(NCS_2)_2$ + COC_3H_7 + ½ Sb_2S_3 B	180 °C B	Endothermic B
II	215–440 A, 220–345 B	47.59/47.30/A	½ Sb_2S_3 + –NC– A	275 °C A	Endothermic A
		23.35/23.36/B	½ Sb_2S_3 + ¼ C_2S B	280 °C B	Endothermic B
III	440–600 A,345–460 B	70.79/70.73/A,1.82/1.73/B	½ Sb_2S_3 A, ½ Sb_2S_3 + –¼ S– B	–	–
IV	460–600 B	72.89/71.37/B	½ Sb_2S_3 B	–	–
Total loss percent = 70.79 A			Remaining material = [½ Sb_2S_3] A = 29.21/30.90/A		
Total loss percent = 72.89 B			Remaining material = [½ Sb_2S_3] A = 27.31/30.90/B		

A = $[(CH_2CH_2)_2NCS_2]_2SbS_2COCH_2CH_2CH_3$

B = $[(CH_2CH_2)_2NCS_2]_2SbS_2COCH(CH_3)_2$

during decomposition of complex is endothermic. Similarly in case of complex $[(CH_2CH_2)_2NCS_2]_2SbS_2COCH(CH_3)_2$ first endothermic peak obtained at 180 °C and another sharp peak obtained at 280 °C temperature in Fig. 2, also indicates that type of reaction during weight losses are endothermic. In case of both complexes first endothermic peak appears as a broad peak which shows loss of organic part of ligand which is not thermally stable such type of peak also arise from dehydration reaction while a sharp endothermic peak which we obtained later in both complexes show change in crystallinity or fusion process. Physical changes usually result in endothermic curve and chemical reactions particularly of oxidative nature are mostly exothermic [28].

FAB^+ mass spectral studies

FAB^+ mass spectra of few of the synthesized complexes, namely, $[(CH_2CH_2)_2NCS_2]_2SbS_2COCH_2CH_2CH_3$ and $[(CH_2CH_2)_2NCS_2]_2SbS_2COCH(CH_3)_2$ have been recorded and possible assignments of the fragments with relative abundance and their *m/z* ratio have been shown in Table 5 and 6, respectively. It follows the similar fragmentation pattern as reported in earlier complexes [30]. Spectrum contains neither

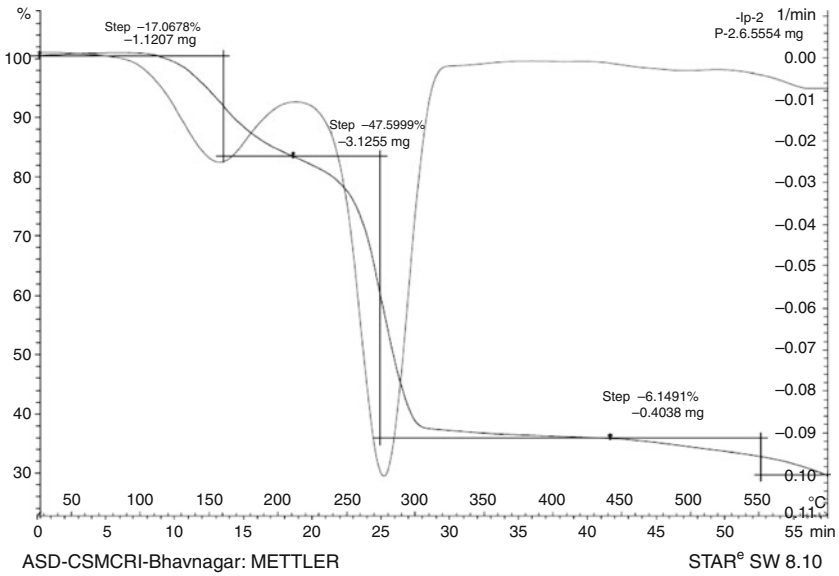

Fig. 1 TG and DTA curve of antimony(III) bis(pyrrolidinedithiocarbamato) *n*-propyldithiocarbonate

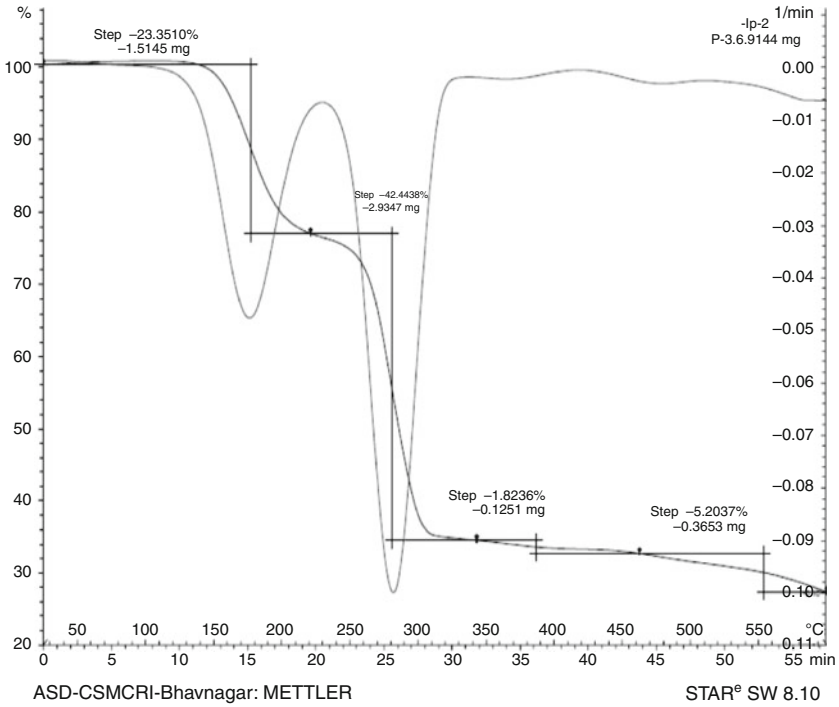

Fig. 2 TG and DTA curve of antimony(III) bis(pyrrolidinedithiocarbamato)iso-propyldithio carbonate

any peak higher than the monomer nor any peak arising from polyantimony species which may exclude the possibility of molecular association in these complexes [36]. Generally complexes of antimony depict no detectable molecular ion peak [37] yet we get a weak molecular ion peak in case of complex$[(CH_2CH_2)_2NCS_2]_2SbS_2COCH(CH_3)_2$ absence of molecular ion peak may be due to pyrolytic decomposition because of relatively high temperature or due to the fragmentation of the molecular ion in the ionization chamber [38], base peak of both complexes for $(CH_2CH_2)_2NCS_2^+$ fragment and in addition to this major fragmentation obtained for dithiocarbamate group rather than xanthate whose fragments doesn't appear after three to fourth step of fragmentation which shows that the xanthate ligand is weaker chelating agent than dithiocarbamate [30]. The fragmentation of complex appears to start with sequential loss of alkyl group from xanthate to dithiocarbamate [39].

Powder X-ray diffraction and SEM studies

Powder X-ray diffraction pattern of two of the synthesized complexes $[(CH_2CH_2)_2NCS_2]_2SbS_2COCH_2CH_2CH_3$ and $[(CH_2CH_2)_2NCS_2]_2SbS_2COCH(CH_3)_2$ have been analyzed on the basis of earlier reported data [29] and shown in

Table 5 FAB^+ mass spectral data of antimony(III) bis(pyrrolidinedithiocarbamato)*n*-propyldithiocarbonates

S·No.	Mass no. *m/z*	Relative abundance /%	Possible formula of the fragments
1.	546	10	$[(CH_2CH_2)_2NCS_2]_2SbS_2COC_3H_4^+$
2.	534	20	$[(CH_2CH_2)_2NCS_2]_2SbS_2COC_2H_4^+$
3.	532	12	$[(CH_2CH_2)_2NCS_2]_2SbS_2COC_2H_2^+$
4.	518	15	$[(CH_2CH_2)_2NCS_2]_2SbS_2COC^+$
5.	412	92	$[(CH_2CH_2)_2NCS_2SbS_2CN(CH_2–CH_2–CH_2–C]^+$
6.	400	12	$[(CH_2CH_2)_2NCS_2SbS_2CN(CH_2–CH_2–CH_2)]^+$
7.	384	15	$[(CH_2CH_2)_2NCS_2SbS_2CN(CH_2–C)]^+$
8.	300	30	$(CH_2CH_2)_2NCS_2SbS^+$
9.	268	30	$(CH_2CH_2)_2NCS_2Sb^+$
10.	147	100	$(CH_2CH_2)_2NCS_2^+$
11.	115	75	$(CH_2CH_2)_2NCS^+$
12.	107	15	$(C–C)_2NCS^+$

Table 6 FAB^+ mass spectral data of antimony(III) bis(pyrrolidinedithiocarbamato)iso-propyldithiocarbonates

S.No.	Mass No. *m/z*	Relative abundance /%	Possible formula of the fragments
1.	549	10	$[(CH_2CH_2)_2NCS_2]_2SbS_2COC_3H_7^i$
2.	534	20	$[(CH_2CH_2)_2NCS_2]_2SbS_2COCH–CH_3^+$
3.	532	18	$[(CH_2CH_2)_2NCS_2]_2SbS_2COCH–CH^+$
4.	490	5	$[(CH_2CH_2)_2NCS_2]_2SbS_2C^+$
5.	412	30	$(CH_2CH_2)_2NCS_2SbS_2CN(CH_2–CH_2–CH_2–C)^+$
6.	400	15	$(CH_2CH_2)_2NCS_2SbS_2CN(CH_2–CH_2–CH_2)^+$
7.	398	10	$(CH_2CH_2)_2NCS_2SbS_2CN(CH_2–CH_2–C)^+$
8.	384	8	$(CH_2CH_2)_2NCS_2SbS_2CN(CH_2–C)^+$
9.	300	10	$(CH_2CH_2)_2NCS_2SbS^+$
10.	268	30	$(CH_2CH_2)_2NCS_2Sb^+$
11.	147	100	$(CH_2CH_2)_2NCS_2^+$
12.	115	30	$(CH_2CH_2)_2NCS^+$
13.	107	8	$(C–C)_2NCS^+$

Tables 7 and 8. Complexes have monoclinic crystal lattice with unit cell volume $V = 1026.96 \times 10^{-8}$ and $V = 1234 \times 10^{-8}$ cm^3, respectively, for both complexes and are polycrystalline in nature, particle size obtained by Scherrer formula shows that nanorange particle formed having particle size 68 and 61 nm for complexes $[(CH_2CH_2)_2NCS_2]_2SbS_2COCH_2CH_2CH_3$ and $[(CH_2CH_2)_2NCS_2]_2SbS_2COCH(CH_3)_2$, respectively. In some cases deviation between the calculated and observed value of interplanar distance (*d*) may exceed up to two as observed in Table 7 which shows that synthesized complexes are in multiphase,

Table 7 The experimental data and the calculated results for powder X-ray diffraction pattern of antimony(III) bis(pyrrolidinedithiocarbamato)*n*-propyldithiocarbonates

2θ/°	*d* spacing in Å observed	*d* spacing in Å calculated	Relative intensity/%	*hkl*
7.58	11.66	14.01	19.09	100
9.52	9.28	8.00	100	110
12.13	7.29	7.10	18.84	200
15.27	5.79	5.55	10.01	002
18.52	4.78	5.18	15.80	111
20.02	4.43	4.80	7.00	210
21.33	4.16	4.23	3.54	012
23.07	3.85	2.77	34.40	320
24.30	3.66	3.83	6.13	310
25.15	3.54	3.70	1.07	003
27.29	3.26	3.24	6.45	31-2
28.65	3.11	3.10	5.26	113
30.08	2.97	3.08	7.39	312
30.63	2.91	2.89	6.99	402
31.80	2.81	2.79	4.44	41-2
33.12	2.70	2.59	6.85	313
33.71	2.65	2.67	9.90	104
34.12	2.62	2.81	9.27	022
36.61	2.45	2.26	4.59	40-4
38.02	2.36	2.32	3.24	304
39.01	2.30	2.36	4.97	600
43.33	2.08	2.09	2.67	12-4
46.24	1.96	2.15	1.58	51-4

Lattice parameters calculated $a = 14.19$ Å, $b = 6.52$ Å, and $c = 11.1$ Å; Angle $\beta = 94.28°$

Unit volume of cell $V = 1026.96 \times 10^{-8}$ cm^3, Particle size of complex 68 nm

as we synthesized mixed ligand complexes which have characteristics of both ligands as observed in X-ray diffraction pattern of both complexes in Figs. 3 and 4, respectively. We obtained interplanar distances matched with both dithiocarbamate and xanthate ligands, have standard diffraction card JCPDS 44-1893, 42-1821, and 37-1565. Monoclinic crystal lattice shows that complexes have lower symmetry which is due to complex nature and lone pair of electron present on antimony which does not take part in bonding and results in distorted geometry of complex. On the other hand Scanning Electron Microscopic studies have been done which image the sample surface by scanning it with a high-energy beam of electrons in a raster scan pattern, i.e., the rectangular pattern of image capture and reconstruct it.

In the case of complex $[(CH_2CH_2)_2NCS_2]_2SbS_2COCH_2CH_2CH_3$ rod shaped particles formed which appears agglomerates in some places under magnification

Table 8 The experimental data and the calculated results for powder X-ray diffraction pattern of antimony(III) bis(pyrrolidinedithiocarbamato)iso-propyldithiocarbonates

2θ/°	*d* spacing in Å observed	*d* spacing in Å calculated	Relative intensity/%	*hkl*
7.78	11.41	11.47	10.63	100
9.54	9.25	7.30	100	110
15.30	5.79	5.79	3.91	002
16.98	5.20	4.94	3.93	102
17.1	5.17	6.32	8.64	11-1
18.96	4.67	4.66	5.38	020
19.64	4.50	4.47	4.22	21-1
20.34	4.35	4.34	3.23	120
23.36	3.81	3.56	9.29	11-2
27.24	3.28	3.41	3.85	112
28.48	3.13	2.54	4.45	322
30.48	2.93	2.42	2.72	402
31.10	2.87	2.94	3.29	320
32.66	2.74	2.73	3.13	230
33.88	2.65	2.77	2.69	104
34.24	2.62	2.67	3.80	23-1
35.96	2.50	3.02	4.99	302
36.02	3.93	2.49	2.63	231
39.56	2.28	2.29	2.82	140

Lattice parameters calculated $a = 11.41$ Å, $b = 9.34$ Å, and $c = 11.58$ Å; Angle $\beta = 96.65°$

Unit volume of cell $V = 1234 \times 10^{-8}$ cm^3, Particle size of complex 61 nm

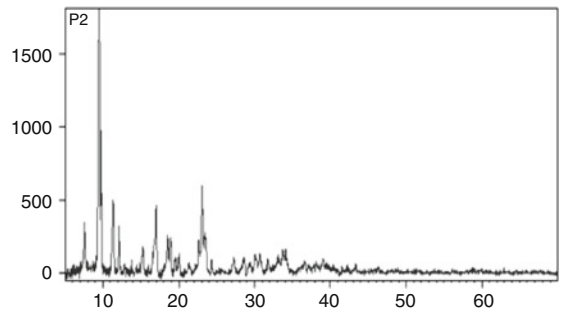

Fig. 3 Powder X-ray diffraction pattern of antimony(III) bis(pyrrolidinedithiocarbamato)*n*-propyldithiocarbonate

of ×450–50 μm. Their shape appears clearly under deep magnification of ×2500–10 μm as shown in Fig. 5 while rough surface appears in complex $[(CH_2CH_2)_2NCS_2]_2SbS_2COCH(CH_3)_2$ in both magnifications which depicts crystalline nature of the complex as shown in Fig. 6.

X-ray diffraction studies help us to understand structural characteristics like crystal lattice, lattice parameters, lattice angle, unit cell volume and particle size of the complex

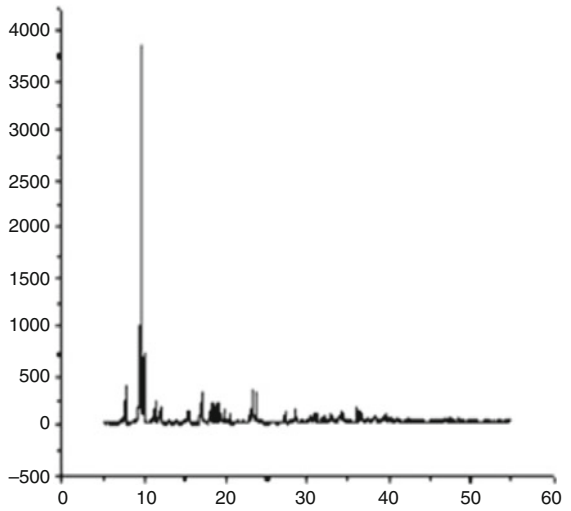

Fig. 4 Powder X-ray diffraction pattern of antimony(III) bis(pyrrolidinedithiocarbamato)iso-propyldithiocarbonate

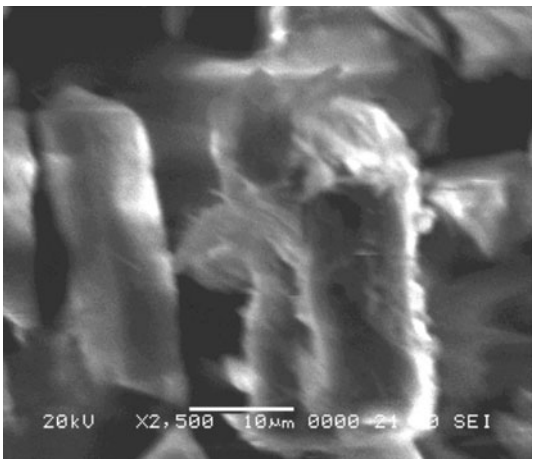

Fig. 5 SEM image of complex antimony(III) bis(pyrrolidinedithiocarbamato)*n*-propyldithiocarbonate at a magnification of ×2500–10 μm

while SEM studies show external morphology contains surface properties thus powder XRD in combination to SEM studies gives characteristic information about complex by which may elaborate more about structural chemistry of the complex.

Structural elucidation

In IR spectra of all antimony complexes presence of distinct signal in the region 1030–1043 cm^{-1} due to *ν*(C–S) stretching vibrations which is due to both pyrrolidinedithiocarbamate and alkyldithiocarbonate moieties indicate

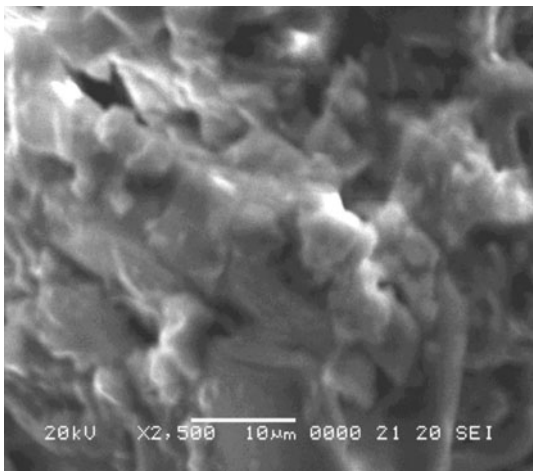

Fig. 6 SEM image of complex antimony(III) bis(pyrrolidinedithiocarbamato)isopropyldithiocarbonate at a magnification of ×2500–10 µm

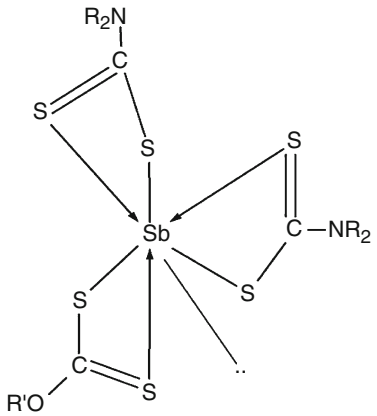

Fig. 7 Schematic molecular representation of antimony(III) bis (pyrrolidinedithiocarbamato)alkyldithiocarbonate(Where R_2 = $(CH_2 CH_2)_2$ and R′ = methyl, ethyl, *n*-propyl, iso-propyl, *n*-butyl, and iso-butyl)

the anisobidentate nature of both ligands to the metal where one of the sulfur atom is weakly coordinated, thus leading to a distorted octahedral geometry with a stereochemically active lone pair of electrons occupying one of the triangular face of the octahedral Fig. 7. Distorted octahedral geometry have also been supported by monoclinic crystal system which also indicates lower symmetry of the complex thus in addition to IR spectral studies powder X-ray diffraction and SEM studies of the complex shows that synthesized complexes are crystalline in nature, rough surface, nanorange particle size and having distorted octahedral geometry with monoclinic crystal system.

Acknowledgements We thank the Sophisticated Analytical Instrumentation Facility (SAIF) of Central Drug Research Institute (CDRI), Lucknow, India for elemental analysis and FAB^+ mass spectral studies. We are also thankful to SAIF, Chandigarh and SAIF, Mumbai, India for providing powder X-ray diffraction and far-IR spectral studies, respectively, and Indian Institute of Science, Bangalore, India for NMR (^1H and ^{13}C) spectral studies.

References

1. Botelho JR, Gondim AD, Santos IMG, Dunstan PO, Souza AG, Fernandes VJ Jr, Araujo AS. Thermochemical parameters of dimethyl and di-iso-propyldithiocarbamate complexes of palladium (II). J Therm Anal Calorim. 2004;75:607–13.
2. Airoldi C, Chagas AP. Some features of the thermochemistry of coordination compounds. Coord Chem Rev. 1992;119:29–65.
3. Souza AG, Neto Souza F, Souza JH, Macedo RO, Oliveria JBL, Pinheiro CD. Thermochemical parameters of complexes of di-isobutyl dithiocarbamate with phosphorus- group elements. J Therm Anal Calorim. 1997;49:679–84.
4. Mahajan K, Fahmi N, Singh RV. Synthesis, characterization and antimicrobial studies of Sb(III) complexes of substituted thioimines. Indian J Chem. 2007;46A:1221–5.
5. Patole J, Padhye S, Newton CJ, Ansor C, Powell AK. Synthesis, characterization and in vitro anticancer activities of semicarbazone and thiosemicarbazone derivatives of salicylaldehyde and their copper complex against human breast cancer cell line MCF-7. Indian J Chem. 2004;43A:1654–8.
6. Feng M-L, Xie Z-L, Huang X-Y. Two gallium antimony sulfides built on a novel heterometallic cluster. Inorg Chem. 2009;48:3904–6.
7. Yao H-G, Min Ji, Ji S-H, Zhang R-C, An Y-L, Ning G-L. Solvothermal synthesis of two novel layered quaternary silver–antimony(III) sulfides with different strategies. Cryst Growth Des. 2009;9:3821–4.
8. Manuel AV, De silva R, Filipa A, Santos LOM. Thermochemical properties of two nitrothiophene derivatives. J Therm Anal Calorim. 2010;100:403–11.
9. Morais C, Pat B, Gobe G, Johnson DW, Healy H. Pyrrolidine dithiocarbamate exerts anti-proliferative and pro-apoptotic effects in renal cell carcinoma cell lines. Nephrol Dial Transplant. 2006;21:3377–88.
10. Morais C, Gobe G, Johnson DW, Healy H. Anti-angiogenic actions of pyrrolidine dithiocarbamate, a nuclear factor kappa B inhibitor. Angiogenesis. 2009;12:365–79.
11. Teke Z, Aytekin FO, Kabay B, Yenisey C, Aydin C, Tekin K, Sacar M, Ozden A. Pyrrolidine dithiocarbamate prevents deleterious effects of remote ischemia/reperfusion injury on healing of colonic anastomoses in rats. World J Surg. 2007;31:1835–42.
12. Zhao J, Shao Z, Zhang X, Ding R, Xu J, Ruan J, Zhang X, Wang H, Sun X, Huang C. Suppression of perfluoroisobutylene induced acute lung injury by pretreatment with pyrrolidine dithiocarbamate. J Occup Health. 2007;49:95–103.
13. Bakbardina OV, Pukhnyarskaya IY, Gazalieva MA, Fazylov SD, Makarov EM. Synthesis and fungicidal activity of *S*-amino derivatives of *O*-alkyldithiocarbonic acids. Russ J Appl Chem. 2006;79:1726–8.
14. Alijanianzadeh M, Saboury AA. Temperature dependence of activation and inhibition of mushroom tyrosinase by ethyl xanthate. Bull Korean Chem Soc. 2007;28:758–62.
15. Ge R, Sun H. Bioinorganic chemistry of bismuth and antimony: target sites of metallodrugs. Acc Chem Res. 2007;40:267–74.
16. Mahajan K, Swami M, Singh RV. Russ J Coord Chem. 2009;35:179–85.
17. Chaudhari KR, Wadawale AP, Ghoshal S, Chopade SM, Sagoria VS, Jain VK. Antimony and bismuth dithiocarboxylates: synthesis, characterization, crystal structures of $[Sb(S_2Ctol)_3]$ and

[$Bi(S_2Cph)_3$] and their transformation to polycrystalline M_2S_3 (M = Sb, Bi). Inorg Chim Acta. 2009;362:1819–24.
18. Hu H, Mo M, Yang B, Zhang X, Li Q, Yu W, Qian Y. Solvothermal synthesis of Sb2S3 nanowires on a large scale. J Cryst Growth. 2003;258:106–12.
19. Desai JD, Lokhande JD. Chemical deposition of Bi_2S_3 thin films from thioacetamide bath. Mater Chem Phys. 1995;41:98–103.
20. Kutasov VA, Lukyanova LN. Thermoelectric properties of multicomponent solid solutions based on bismuth and antimony chalcogenides with n-type conduction in the region of impurity and mixed conduction. Phy Solid State. 2006;48:2289–94.
21. Arivuoli D, Gnanam FD, Ramasamy P. Growth and microhardness studies of chalcogenides of arsenic, antimony and bismuth. J Mater Sci Lett. 1988;7:711–3.
22. Luan SR, Zhu YH, Jia YQ, Cao Q. Characterization and thermal analysis of thiourea and bismuth trichloride complex. J Therm Anal Calorim. 2010;99:523–30.
23. Wu J, Chen S-P, Di Y-Y, Gao S-L. Low-temperature thermodynamics of $Ln(Me_2dtc)_3(C_{12}H_8N_2)$($Me_2dtc$ = dimethyldithiocarbamate, Ln = La, Pr, Nd, Sm). J Therm Anal Calorim. 2010; 100:1091–8.
24. Li X, Wu Y, Gu D, Gan F. Synthesis spectral and thermal properties of some transition metal(II) complexes with a novel ligand derived from thiobarbituric acid. J Therm Anal Calorim. 2009;98:387–94.
25. Chauhan HPS, Shaik NM, Singh UP. Synthesis, spectroscopic characterization and in vitro studies of antimicrobial activity of bis(diorganodithiocarbamato)organodithiocarbonatobismuth(III) complexes. Appl Organomet Chem. 2006;20:142–8.
26. Chauhan HPS, Singh UP. Synthetic, spectral, thermal and antimicrobial studies on some bis(*N, N′*-dialkyldithiocarbamato)antimony(III) alkylenedithiophosphates. Appl Organomet Chem. 2007; 21:880–9.
27. Riddick JA, Bunger WB. Techniques of chemistry (organics solvents). 3rd ed. New York: Wiley InterScience; 1970.
28. Vogel AI. A textbook of quantitative chemical analysis. 6th ed. India: Saurabh Printers; 2008.
29. Chauhan HPS, Bakshi A, Bhatiya S. Synthetic, spectral as well as in vitro antimicrobial studies on some bismuth(III) bis(N, N-dialkyldithiocarbamato)alkylenedithiophosphates. Appl Organomet Chem. 2010;24:317–25.
30. Kheiri FMN, Tsipis CA, Manoussakis GE. Synthesis and spectroscopic study of some new mixed-ligand Bi(III) 1, 1-dithiolate complexes. Inorg Chim Acta. 1977;25:223–7.
31. Manoussakis GE, Tsipis CA. Preparation and study of some arsenic and antimony tris dithiocarbamates. J Inorg Nucl Chem. 1973;35:743–50.
32. Manoussakis GE, Tsipis CA, Hadjikostas CC. Five-coordinate bromobis(dialkyldithiocarbamate) complexes of arsenic, antimont and bismuth. Can J Chem. 1975;53:1530–5.
33. Garje SS, Jain VK. Chemistry of arsenic, antimony and bismuth compounds derived from xanthate, dithiocarbamate and phosphorus based ligands. Coord Chem Rev. 2003;236:35–56.
34. Chauhan HPS, Kori K, Shaik NM, Singh UP. Complexes of bis(dialkyldithiocarbamato) arsenic(III) with alkyldithiocarbonates: synthesis and characterization. Main Group Met Chem. 2004;27:11–9.
35. Chauhan HPS, Singh UP. Synthetic, spectral, thermal and antimicrobial studies of bis(N, N-dialkyldithiocarbamato)arsenic(III) and antimony(III) complexes with diphenyldithiophosphate and diphenyldithiophosphinate. Appl Organomet Chem. 2006;20: 404–10.
36. Gupta RK, Rai AK, Mehrotra RC. Mixed chloride xanthates of phenyl-arsenic and -antimony(III). Indian J Chem. 1985;24A: 752–4.
37. Tsipis CA, Manoussakis GE. Synthesis and spectral study of new iodobis(dialkyldithiocarbamate) complexes of arsenic, antimony and bismuth. Inorg Chim Acta. 1976;18:35–45.
38. Gupta RK, Rai AK, Mehrotra RC, Jain VK. Cyclic *O*, *O*-alkylenedithiophosphates of phenyl-arsenic and -antimony. Inorg Chim Acta. 1984;88:201–7.
39. Gupta RK, Rai AK, Mehrotra RC, Jain VK. Alkylxanthates of phenylarsenic(III). Polyhedron. 1984;3:721–8.